Precision Asteroseismology
Proceedings IAU Symposium No. 301, 2013
J. A. Guzik, W. J. Chaplin, G. Handler & A. Pigulski, eds.

doi:10.1017/S1743921313014373

Iron-group opacities in the envelopes of massive stars

Maëlle Le Pennec and Sylvaine Turck-Chièze

CEA/DSM/IRFU/SAp, CE Saclay, 91191 Gif-sur-Yvette, France
email: maelle.le-pennec@cea.fr; Sylvaine.Turck-Chieze@cea.fr

Abstract. β Cephei and SPB stars are pulsating stars for which the excitation of modes by the κ mechanism, due to the iron-group opacity peak, seems puzzling. We have first investigated the origins of the differences noticed between OP and OPAL iron and nickel opacity calculations (up to a factor 2), a fact which complicates the interpretation. To accomplish this task, new well-qualified calculations (SCO-RCG, HULLAC and ATOMIC) have been performed and compared to values of these tables, and most of the differences are now well understood. Next, we have exploited a dedicated experiment on chromium, iron and nickel, conducted at the LULI 2000 facilities. We found that, in the case of iron, detailed calculations (OP, ATOMIC and HULLAC) show good agreement, contrary to all of the non-detailed calculations. However, in the case of nickel, OP calculations show large discrepancies with the experiments but also with other codes. Thus, the opacity tables need to be revised in the thermodynamical conditions corresponding to the peak of the iron group. Consequently we study the evolution of this iron peak with changes in stellar mass, age, and metallicity to determine the relevant region where these tables should be revised.

Keywords. opacity, atomic data, atomic processes, stars: oscillations

1. Introduction

The κ mechanism is responsible for the pulsation of stars between 1.6 to 20 $M_\odot$. For massive stars (2.5 to 20 $M_\odot$), this mechanism is due to M-shell transitions for the elements of the iron group (chromium, iron, nickel and copper) which induce an opacity bump. SPB and β Cephei stars are examples of such pulsating stars. β Cephei ($M > 8\,M_\odot$) are particularly interesting because they will evolve into supernovae and thus are linked to our understanding of the interstellar medium enrichment. However, they are particularly poorly understood. Indeed, there are, for instance, some difficulties interpreting the pulsations of these stars, as one observes modes which were calculated to be stable in theoretical predictions using OP or OPAL opacity tables (Pamyatnykh 1999, Zdravkov & Pamyatnykh 2009). Furthermore, depending on the mass of the star, some of the modes seem better predicted using OP (Seaton & Badnell 2004) or OPAL (Rogers & Iglesias 1992) tables. This fact suggests that some of these opacities could be inaccurately determined for both tables (Daszyńska-Daszkiewicz & Walczak 2010) or that some hydrodynamic process plays an important role not yet understood. We are studying in this paper the first possibility: an inaccurate determination of the iron opacity bump. To deal with this problem, several activities have been developed at CEA in France to improve the present situation: new calculations have been developed and compared to understand the differences, and two XUV campaigns of experiments have been conducted at the LULI 2000 facility for the different elements at temperature around 25 eV and density of about 2 mg cm^{-3}.

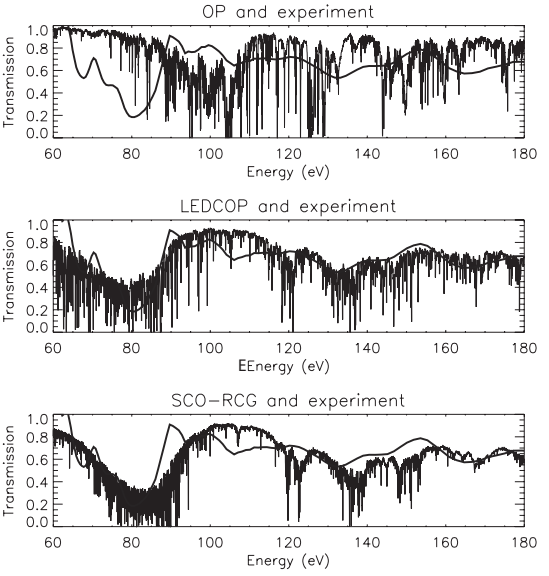

Figure 1. Comparison between nickel transmission spectrum (linked to the opacity through an exponential) taken at LULI 2000 (thick continuous line) and respectively OP, LEDCOP and SCO-RCG. The OP and SCO-RCG calculations are given at 27 eV, 3.4 mg cm^{-3} and LEDCOP at 26 eV, 2 mg cm^{-3}. The domain 60 – 180 eV (700 000 K – 2×10^6 K) is the domain where the Rosseland mean is the most important. From Turck-Chièze *et al.* (2013).

2. Calculations and experiments

Opacity codes are based on different approaches (Turck-Chièze *et al.* 2011): statistical (STA, SCO), detailed (OP, HULLAC, Bar-Shalom *et al.* 2001; ATOMIC, Magee *et al.* 2004; LEDCOP, OPAS) or mixed (SCO-RCG). The two major contributors to the iron bump are iron and nickel, so the calculations have been performed for these two elements as highest priority. Comparisons have been made for tabulated temperature and density values near the experimental ones. These comparisons show that detailed calculations tend to agree, except for the OP results (Gilles *et al.* 2011). The interaction of configuration plays an important role for iron in this domain of temperature and density, and largely explains the difference from the statistical calculations (Gilles *et al.* 2012). For OP, in the case of iron, the Rosseland mean values show differences of around 6 – 7% with ATOMIC and HULLAC, but up to 40% with statistical calculations. In the case of nickel, OP differs clearly from the other codes, showing discrepancies of at least 50% (Turck-Chièze *et al.* 2013).

Figure 1 presents the first analysis of the experiment on nickel (Turck-Chièze *et al.* 2013) compared to different code results (OP, LEDCOP and SCO-RCG). The OP calculations, in fact extrapolated from iron, disagree strongly with the experiments and other calculations. This result confirms some conclusions of Salmon *et al.* (2012). New OP, HULLAC and ATOMIC calculations are in progress, but take a very long time to perform. One concludes that the origin of the differences between OP and OPAL is of different nature for iron and nickel.

3. Study of the iron bump

We have calculated numerous stellar models to determine the domain where new calculations need to be performed. For this task, we have explored how the iron peak varies

https://doi.org/10.1017/S1743921313014373 Published online by Cambridge University Press

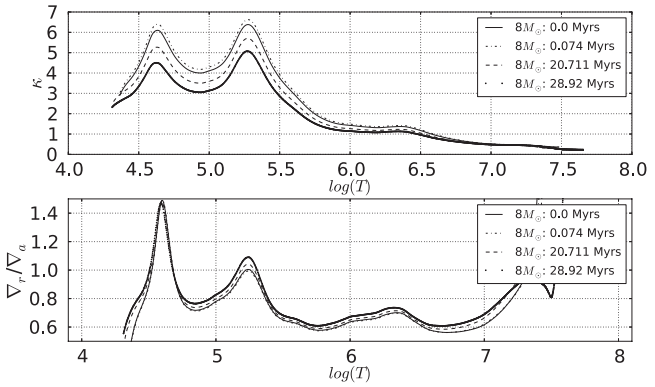

Figure 2. Age variation of the amplitude of the iron bump. Top panel: Opacity in $\mathrm{cm}^2\,\mathrm{g}^{-1}$ versus $\log T$ in the case of a $8\,M_\odot$ star. The first bump at $\log T = 4.6$ is linked to partially ionized helium, the second at 5.25 is the iron bump and the third at 6.3 is the deep iron bump, linked to L-shell bound-free transitions of iron. Bottom panel: ratio $\nabla_\mathrm{r}/\nabla_\mathrm{a}$ versus $\log T$.

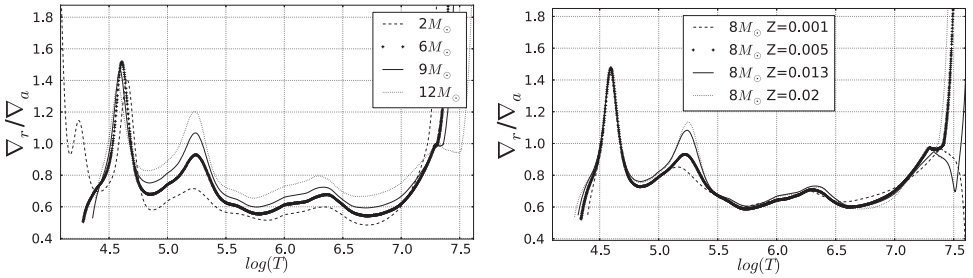

Figure 3. *Left*: Influence of the mass on the amplitude of the iron bump. *Right*: Influence of the metallicity on the iron bump for an $8\,M_\odot$ star. The ratio of the two gradients is always around one so, depending on the properties of stars, convective instability can appear.

with mass, age and metallicity during the main sequence of SPB and β Cep stars. All models were calculated using the stellar evolution code MESA (Paxton *et al.* 2011) and the OPAL opacity tables with the AGSS09 (Asplund *et al.* 2009) abundance mixture. Figure 2 shows that opacity uncertainties during the stellar lifetime have large consequences on the stability of the acoustic modes. Adopting the Schwarzschild criterion to see the onset of the convective instability (ratio of the radiative gradient to the adiabatic gradient greater than 1), one observes that this ratio is very near to 1 at the iron-bump region from one source of opacity calculation to another, and so the resulting structure of the star can be different. In less than 10 Myr, a small convective zone appears in the iron bump region of an $8\,\mathrm{M}_\odot$. Precise knowledge of the age of the star is needed to correctly predict the observed modes.

Figure 3 shows the influence of mass and metallicity on the iron bump. The gradient ratio varies rapidly with mass and metallicity, and is around 1 for these types of stars, so a precise knowledge of the opacity is required to properly determine the theoretical frequencies.

This study allows us to determine the thermodynamical conditions in which the iron-peak opacity must be carefully estimated for stars between 2 to $20\,M_\odot$. It is known that opacities vary rapidly with temperature, so one can notice that this peak appears always at the same position independently of the chosen conditions between 100 000 K to 320 000 K. However, the free electron density, N_e, principally due to the totally ionized

https://doi.org/10.1017/S1743921313014373 Published online by Cambridge University Press

Table 1. Domain of investigation of the iron bump for stars from 2.5 to 20 $M_\odot$ and $Z = 0.02$. The free electron density decreases with stellar mass. The present domain will be reduced for specific analyses, and the study extended to the Magellanic Clouds.

Mass	$N_{\mathrm{e,min}}$ **(cm^{-3})**	$N_{\mathrm{e,max}}$ **(cm^{-3})**
2.5 $M_\odot$	$7.87 \cdot 10^{16}$	$1.57 \cdot 10^{19}$
6 $M_\odot$	$1.93 \cdot 10^{16}$	$3.94 \cdot 10^{18}$
10 $M_\odot$	$8.63 \cdot 10^{15}$	$1.98 \cdot 10^{18}$
14 $M_\odot$	$4.63 \cdot 10^{15}$	$1.22 \cdot 10^{18}$
20 $M_\odot$	$2.43 \cdot 10^{15}$	$7.69 \cdot 10^{17}$

helium and hydrogen at these temperatures, varies with mass:

$$N_{\mathrm{e}} = \rho \sum_i \frac{Q_i \chi_i}{A_i}.$$

Q_i is the ionization charge, χ_i the relative contribution in mass, A_i the atomic weight of species i and ρ is the density.

4. Conclusion

The OPAC consortium studies (new calculations and new experiments) help to understand the discrepancies between OP and OPAL in the iron bump which excites the modes of β Cephei and SPB stars. Iron opacities are better estimated by OP calculations at relatively high temperature but OP nickel opacities are not correct for all the considered cases. As the iron group peak varies strongly with age, mass and composition of the star, the properties of the stars need to be correctly known and the opacities of the different elements of the iron group must be precisely calculated for a range of T and N_{e} that we are determining. New tables are in construction thanks to the HULLAC, ATOMIC and SCO-RCG codes, and we hope for results in 2014. At that time, radiative acceleration and non LTE-conditions will also be investigated.

References

Asplund, M., Grevesse, N., Sauval, A. J., & Scott, P. 2009, *ARAA*, 47, 481
Bar-Shalom, A., Klapisch, M., & Oreg, J. 2001, *J. Quant. Spectrosc. Radiat. Transf.*, 71, 169
Daszyńska-Daszkiewicz, J. & Walczak, P. 2010, *MNRAS*, 403, 496
Gilles, D., Turck-Chièze, S., Loisel, G., *et al.* 2011, *High Energy Density Physics*, 7, 312
Gilles, D., Turck-Chièze, S., Busquet, M., *et al.* 2012, in *ECLA 2011*, vol. 58, EAS Pub. Ser., p. 51
Magee, N. H., Abdallah, J., Colgan, J., *et al.* 2004, *AIP-CS*, 730, 168
Paxton, B., Bildsten, L., Dotter, A., *et al.* 2011, *ApJS*, 192, 3
Pamyatnykh, A. A. 1999, *AcA*, 49, 119
Rogers, F. J. & Iglesias, C. A. 1992, *ApJS*, 79, 507
Salmon, S., Montalbán, J., Morel, T., *et al.* 2012, *MNRAS*, 422, 3460
Seaton, M. J. & Badnell, N. R. 2004, *MNRAS*, 354, 457
Turck-Chièze, S., The OPAC Consortium 2011a, *J. Phys. Conf. Ser.*, 271, 012035
Turck-Chièze, S., The OPAC Consortium 2011b, *Ap&SS* 336, 103
Turck-Chièze, S., Gilles, D., Le Pennec, M., *et al.* 2013, *High Energy Density Phys.*, 9, 473
Zdravkov, T. & Pamyatnykh, A. A. 2009, *AIP-CS*, 1170, 338

https://doi.org/10.1017/S1743921313014373 Published online by Cambridge University Press